Evidence for octupole collectivity in Pt-172

Ertoprak, A.

2020-02-20

Ertoprak , A , Cederwall , B , Qi , C , Aktas , O , Doncel , M , Hadinia , B , Liotta , R , Sandzelius , M , Scholey , C , Andgren , K , Back , T , Badran , H , Braunroth , T , Calverley , T , Cox , D M , Cullen , D M , Fang , Y D , Ganioglu , E , Giles , M , Gomez Hornillos , M B , Grahn , T , Greenlees , P T , Hilton , J , Hodge , D , Ideguchi , E , Jakobsson , U , Johnson , A , Jones , P M , Julin , R , Juutinen , S , Ketelhut , S , Khaplanov , A , Kumar Raju , M , Leino , M , Li , H , Liu , H , Matta , S , Modamio , V , Nara Singh , B S , Niikura , M , Nyman , M , Ozgur , I , Page , R D , Pakarinen , J , Papadakis , P , Partanen , J , Paul , E S , Petrache , C M , Peura , P , Rahkila , P , Ruotsalainen , P , Saren , J , Sorri , J , Stolze , S , Subramaniam , P , Taylor , M J , Uusitalo , J , Valiente-Dobon , J J & Wyss , R 2020 , ' Evidence for octupole collectivity in Pt-172 ' , European Physical Journal. A, Hadrons and Nuclei , vol. 56 , no. 2 , 65 . https://doi.org/10.1140/epja/s10050-020-00071-6

http://hdl.handle.net/10138/313536
https://doi.org/10.1140/epja/s10050-020-00071-6

Eur. Phys. J. A (2020) 56:65
https://doi.org/10.1140/epja/s10050-020-00071-6

THE EUROPEAN PHYSICAL JOURNAL A

Regular Article - Experimental Physics

Evidence for octupole collectivity in ^{172}Pt

A. Ertoprak[1,2,a], B. Cederwall[1], C. Qi[1], Ö. Aktas[1], M. Doncel[3], B. Hadinia[1], R. Liotta[1], M. Sandzelius[4], C. Scholey[4], K. Andgren[1], T. Bäck[1], H. Badran[4], T. Braunroth[5], T. Calverley[3,4], D. M. Cox[4], D. M. Cullen[6], Y. D. Fang[7], E. Ganioğlu[2], M. Giles[6], M. B. Gomez Hornillos[8], T. Grahn[4], P. T. Greenlees[4], J. Hilton[3,4], D. Hodge[6], E. Ideguchi[7], U. Jakobsson[9], A. Johnson[1], P. M. Jones[4], R. Julin[4], S. Juutinen[4], S. Ketelhut[4], A. Khaplanov[1], M. Kumar Raju[7], M. Leino[4], H. Li[1], H. Liu[1], S. Matta[1], V. Modamio[10], B. S. Nara Singh[6], M. Niikura[11], M. Nyman[4], I. Özgür[2], R. D. Page[3], J. Pakarinen[4], P. Papadakis[4,8], J. Partanen[4], E. S. Paul[3], C. M. Petrache[12], P. Peura[4], P. Rahkila[4], P. Ruotsalainen[4], J. Sarén[4], J. Sorri[4], S. Stolze[4], P. Subramaniam[1], M. J. Taylor[13], J. Uusitalo[4], J. J. Valiente-Dobón[14], R. Wyss[1]

[1] KTH Royal Institute of Technology, 10691 Stockholm, Sweden
[2] Department of Physics, Faculty of Science, Istanbul University, Vezneciler/Fatih, 34134 Istanbul, Turkey
[3] Department of Physics, Oliver Lodge Laboratory, University of Liverpool, Liverpool L69 7ZE, United Kingdom
[4] Department of Physics, University of Jyvaskyla, P.O. Box 35, 40014 Jyvaskyla, Finland
[5] Institut für Kernphysik, Universität zu Köln, 50937 Cologne, Germany
[6] Schuster Building, School of Physics and Astronomy, The University of Manchester, Manchester M13 9PL, United Kingdom
[7] Research Center for Nuclear Physics, Osaka University, Osaka 567-0047, Japan
[8] STFC Daresbury Laboratory, Daresbury, Warrington WA4 4AD, United Kingdom
[9] Department of Chemistry, University of Helsinki, P.O. Box 3, 00014 Helsinki, Finland
[10] Department of Physics, University of Oslo, 0316 Oslo, Norway
[11] CNS, University of Tokyo, Wako 351-0198, Japan
[12] Centre de Sciences Nucléaires et Sciences de la Matière, CNRS/IN2P3, Université Paris-Saclay, 91405 Orsay, France
[13] Division of Cancer Sciences, School of Medical Sciences, The University of Manchester, Manchester M13 9PL, United Kingdom
[14] Istituto Nazionale di Fisica Nucleare, Laboratori Nazionali di Legnaro, 35020 Legnaro, Italy

Received: 10 October 2019 / Accepted: 11 January 2020

Communicated by Robert Janssens

Abstract Excited states in the extremely neutron-deficient nucleus ^{172}Pt were populated via ^{96}Ru(^{78}Kr, $2p$) and ^{92}Mo(^{83}Kr, $3n$) reactions. The level scheme has been extended up to an excitation energy of ≈ 5 MeV and tentative spin-parity assignments up to $I^{\pi} = 18^{+}$. Linear polarization and angular distribution measurements were used to determine the electromagnetic E1 character of the dipole transitions connecting the positive-parity ground-state band with an excited side-band, firmly establishing it as a negative-parity band. The lowest member of this negative-parity structure was firmly assigned spin-parity 3^{-}. In addition, we observed an E3 transition from this 3^{-} state to the ground state, providing direct evidence for octupole collectivity in ^{172}Pt. Large-scale shell model (LSSM) and total Routhian surface (TRS) calculations have been performed, supporting the interpretation of the 3^{-} state as a collective octupole-vibrational state.

1 Introduction

The concept of deformations and shapes in atomic nuclei, based on the observations of large quadrupole moments, rotational band structures and vibrational-like spectra is one of the corner stones of nuclear physics. Most deformed nuclei seem adequately described by an axial- and reflection-symmetric prolate spheroidal shape, and due to its invariance under space inversion, all members of rotational band structures based on it will consequently have the same parity [1]. Deviations from this simple picture, like oblate, triaxial, or higher-order multipole shapes appear, surprisingly, to be quite rare. With the first observations of low-lying negative-parity states in even–even nuclei came also the first evidence for reflection-asymmetric, "pear shaped", nuclei [2–4]. However, extensive investigations of nuclei with low-lying negative-parity structures has led to the conclusion that reflection-asymmetric shapes are not as stable as the familiar quadrupole deformations and quite rare. Still, ample experimental evidence such as interleaved positive- and negative-parity states, large electric dipole and octupole moments, and

[a] e-mail: ertoprak@kth.se (corresponding author)

Published online: 20 February 2020

parity doublets in odd-mass nuclei, support the picture that atomic nuclei may have at least a tendency towards acquiring octupole-deformed shapes. While the current experimental evidence for stable octupole-deformed shapes is rather illusive and the indications of strong ground-state octupole correlations seem limited to ^{224}Ra [5], ^{226}Ra [6], ^{144}Ba [7] and ^{146}Ba [8], the observation of low-lying quantum states in many even–even nuclei with angular momentum and parity $I^{\pi} = 3^{-}$ indicates the presence of octupole vibrations about a reflection-symmetric shape [9]. For even–even nuclei, measurements of the linear polarization to determine the electromagnetic character of the dipole transitions connecting the band structures built on such states with the ground-state band provides crucial evidence for collective octupole correlations [10]. However, E1 transition strengths are not enough for the unambiguous determination of octupole correlations since they can be strongly affected by single-particle contributions [11,12]. More conclusive evidence is provided by a large value of the electric octupole ($E3$) moment for the $3^{-} \rightarrow 0^{+}$ transition to the ground state, indicating collective behaviour of the nucleons [13–16]. Since such transitions are strongly hindered and rarely compete with transitions of lower multipolarity, the observation of an E3 transition to the ground state in an even–even nucleus can often be considered a strong indication of octupole collectivity.

The experimental picture is in general agreement with the theoretical prediction that octupole vibrations or octupole deformation in nuclei is produced by the long-range octupole-octupole interactions between nucleons. Such correlations depend on the Y_{30} matrix elements between single-particle states. Consequently, shapes having octupole deformation will become energetically favored due to $\Delta l = \Delta j = 3$ coupling of single-particle orbitals that lie close to each other and to the Fermi surface. This is predicted to produce the "magic" octupole numbers 34, 56, 88, and 134 [17–19], where, e.g. $N = 134$ lies between the $g_{9/2}$ and $j_{15/2}$ orbitals and $Z = 88$ lies between the $f_{7/2}$ and $i_{13/2}$ orbitals. Since the "octupole magic" numbers are found away from the traditional magic numbers corresponding to the spherical shell gaps such nuclei are generally quadrupole deformed and the maximal octupole correlations can therefore spread out over several nucleon numbers [20].

This paper presents new measurements of excited states in ^{172}Pt, extending the yrast ground-state positive-parity band structure up to ≈ 5 MeV excitation energy. An excited sideband structure has also been extended and its negative parity determined unambiguously.

2 Experimental details

Measuring high-spin states in very neutron-deficient nuclei such as ^{172}Pt, situated 20 neutrons away from the most neutron-deficient stable platinum isotope, presents large challenges. Not only are the production cross sections in fusion-evaporation reactions exceedingly low but the emission of charged particles, neutrons and γ rays from the nuclei of interest is also immersed in a vast "background" from reaction channels close to stability. For cases where characteristic ground-state decays like α decays are available and the half-life is sufficiently short the experimental difficulties can be overcome by using the recoil decay tagging (RDT) technique [21,22]. This highly selective and efficient technique provided clean correlations between the prompt γ rays detected at the target position and the subsequent characteristic α decays of the ^{172}Pt recoils. In the present work, data were obtained from two different experiments performed at the Accelerator Laboratory of the University of Jyväskylä (JYFL), Finland.

In the first experiment, which was primarily used for the level scheme determination, excited states in ^{172}Pt were populated via the ^{96}Ru(^{78}Kr, $2p$) fusion-evaporation reaction. The beam of ^{78}Kr ions was accelerated to energies of 342 and 348 MeV by the K-130 cyclotron and used to bombard a self-supporting, 96% isotopically enriched ^{96}Ru target foil with an areal density of 0.5 mg/cm^2. A carbon foil with a thickness 50 mg/cm^2 was used as a charge reset foil and placed immediately downstream of the target. The total time of irradiation was 320 h with an average beam intensity of 10 pnA. The experimental set-up consisted of the JUROGAM I high-purity germanium detector array [23,24] and the GREAT spectrometer [25], operated in conjunction with the RITU gas-filled recoil separator [26–28]. The recoiling fusion evaporation products were separated from the beam particles and fission products in RITU and were implanted into the two double-sided silicon strip detectors (DSSSD) of GREAT, placed at the focal plane of RITU. The GREAT spectrometer is a composite array comprising two double-sided silicon strip detectors (DSSSD), a multiwire proportional counter (MWPC), an array of 28 Si PIN-diode detectors, one planar and one HPGe clover germanium detector. The DSSSDs have an active area of 60 × 40 mm^2 with a strip pitch of 1 mm in both directions, giving 4800 independent pixels in total. The discrimination of the beam particles from the fusion residues at the focal plane was achieved by measuring the energy loss signal in the MWPC and the time of flight (TOF) between the MWPC and the DSSSDs.

The second experiment was designed primarily for lifetime measurements of excited states in ^{172}Pt [29] using the differential plunger device for unbound nuclear states (DPUNS) [30]. We also used data from the second experiment in order to extract polarization asymmetry and angular

distribution information. ^{83}Kr ions with an energy of 383 MeV were let to impinge on a self-supporting, isotopically enriched ^{92}Mo target mounted inside DPUNS. The ^{172}Pt fusion-evaporation residues were produced in the (^{83}Kr,3n) channel, separated from the beam particles and fission products in RITU, and subsequently implanted into the two double-sided silicon strip detectors (DSSSD) of GREAT. Prompt γ rays that were produced at the target position were detected by the JUROGAM II germanium detector array, consisting of 43 EUROGAM phase-I type [31] germanium detectors. The germanium detectors were arranged into six rings, with angles $\theta = 72°$, 86°, 94°, 108°, 134° and 154° relative to the beam direction.

The data were recorded by the triggerless total data readout (TDR) acquisition system [32] which provides absolute time stamp with an accuracy of 10 ns. In both experiments prompt γ-ray transitions belonging to ^{172}Pt were cleanly selected using delayed coincidences with the characteristic α-decay energies of the ^{172}Pt ground-state decays. The measured γ-ray energies were corrected for Doppler shifts as γ-ray emission occurred while the recoils were in flight ($v/c = 0.045$).

The data were sorted into $E_\gamma - E_\gamma$ matrices using the GRAIN software package [33] and histograms were analysed offline using the RADWARE data analysis package [34].

3 Data analysis

Excited states in ^{172}Pt were first reported by Cederwall et al. [35]. Shortly thereafter, Seweryniak et al. [36] reported the observation of γ rays in ^{172}Pt from an independent measurement and placed them in a slightly different level scheme. Danchev et al. [37] confirmed the observations of Cederwall et al. [35] and extended the ground state band up to tentative spin of 12$\hbar$. The level scheme reported in [37] was later modified and extended by Joss et al. [38]. In the latter work, the levels of the ground-state band were determined up to an excitation energy at 4219 keV. Our results confirm the assignment of all transitions reported by Joss et al. [38] to ^{172}Pt whereas some of their placements in the level scheme have been reevaluated. In the present work, the ground-state band has also been extended with two transitions, from (14^+) to (18^+). The side band, which was previously tentatively assigned as consisting of negative-parity states, is constructed on top of the previously identified (3^-) excited state and extended from (7^-) up to a tentative spin-parity of (19^-). Linear polarization measurements have also been performed for several of the γ rays depopulating excited states in ^{172}Pt for the first time in the present work as well as additional angular distribution measurements. These allowed unambiguous determination of their multipolarities and hence firm spin-parity assignments of some of the states, including the 3^-, 5^-, and 7^- states.

The intensities of the Compton scattered γ rays in the segmented clover detectors of the JUROGAM II array were used to calculate the polarization asymmetry parameter (A) which is proportional to the degree of the linear polarization normalized to the corrected total intensity:

$$A = \frac{I_\perp - I_\parallel}{I_\perp + I_\parallel}. \quad (1)$$

Here $I_\perp$ is the intensity of the perpendicular-scattered photons whereas $I_\parallel$ is the intensity of the parallel-scattered photons with respect to the plane spanned by the direction of the primary γ-ray and the beam direction. Multipolarity assignments have been made for the strongest γ-ray transitions making use of this information together with information from the angular intensity distribution measurements. The angular distribution ratio (R_A) is defined by the ratio of the intensity of γ rays and calculated through this relation:

$$R_A = N\left[\frac{I(\theta \approx 140°)}{I(\theta \approx 90°)}\right] \quad (2)$$

Here N is the normalisation constant to account for the different number of detectors in each ring.

The proposed level scheme deduced from the present work is shown in Fig. 1. The relative intensities of the γ rays (I_γ) are proportional to the widths of the arrows and normalised to the most intense transition at $E_\gamma = 458$ keV (Table 1).

Joss et al. [38] suggested that the 411 keV transition feeds the 6^+ level. However, using the coincidence relationships obtained in the present work, it was found that the 411 keV transition is in coincidence with the 653 keV and 588/587 keV doublet transitions. The state at 2956 keV, which was not seen in earlier measurements, is tentatively assigned as 10^-. There are also some other modifications to the level scheme above the 12^+ and 7^- states compared with the assignments of Joss et al. Coincidence relationships reveal that the 1466 keV transition is in coincidence with the 374 keV transition but not with the $2^+ \rightarrow 0^+$ transition, showing that it directly feeds the ground state. Note that the angular distribution ratio obtained for the 1008 keV transition is identical within a relative experimental uncertainty of around 10% to that of the 769 keV $5^- \rightarrow 4^+$ transition, strongly supporting its assignment as a stretched dipole transition. The 374 keV $5^- \rightarrow 3^-$ transition is assigned as a stretched E2 transition based on its angular distribution ratio with a somewhat larger relative uncertainty of around 30%. These assignments support the 1466 keV state as being of spin-parity 3^- and as the lowest member of the negative-parity structure.

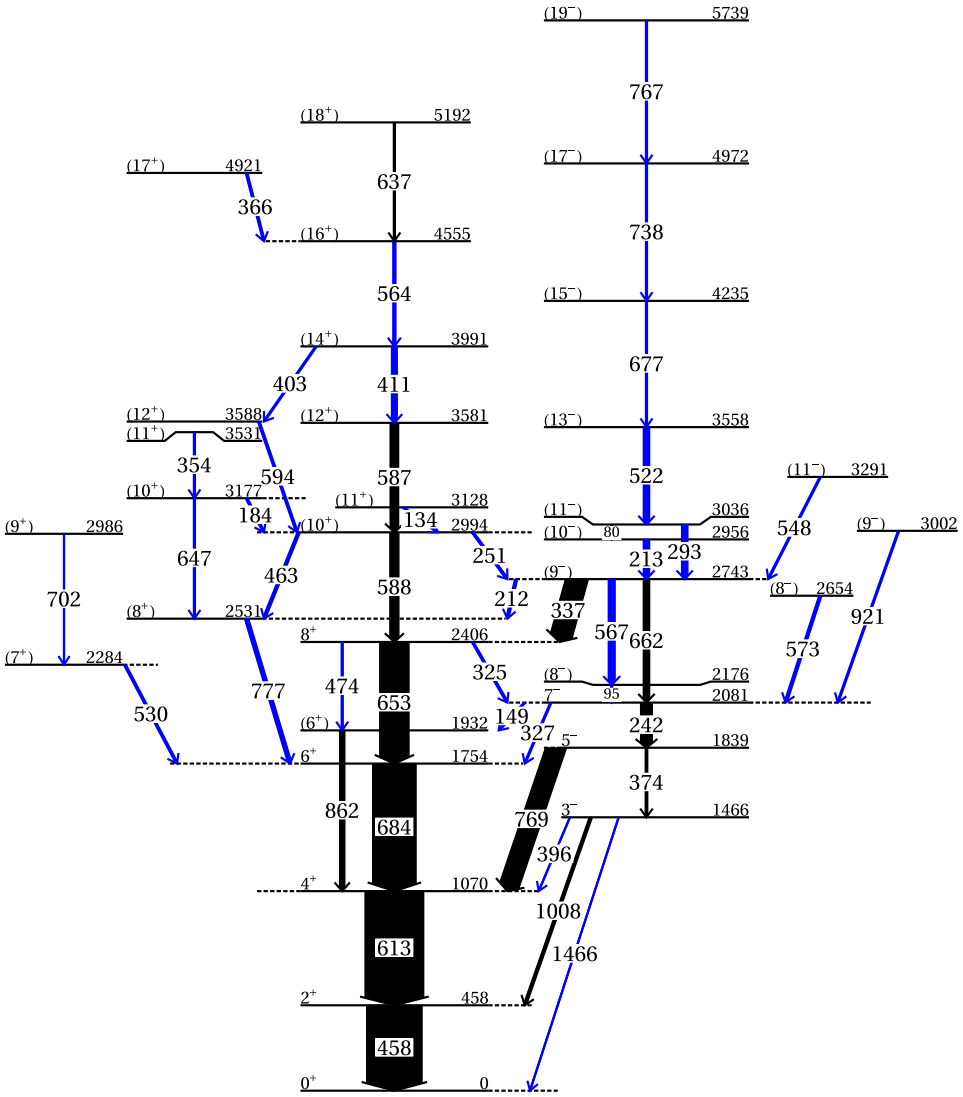

Fig. 1 Level scheme of ^{172}Pt deduced from the present work. The new transitions are marked with blue in the level scheme. Tentative spin-parity assignments are given in brackets

Figure 2a shows the spectrum for the ground state band which was obtained by gating on the 653 keV transition. A γ-ray coincidence spectrum produced by setting a gate on the 213 keV transition is shown in Fig. 2b. It shows all the other γ-ray transitions associated with the negative-parity side band. Compared with the previous work [38], the side band has been extended up to an excitation energy of ~ 6 MeV.

Figure 3 displays the summed energy spectrum for γ rays in coincidence with the 374, 662 and 213 keV transitions. The insets highlight the 1466 keV transition which is assigned as a stretched E3 transition connecting the 3^- state with the 0^+ ground state.

Figure 4 shows the observed linear polarization asymmetry values (A) versus the angular distribution ratios (R_A) for some of the γ-ray transitions belonging to ^{172}Pt. The corresponding values for a few of the known strongest γ-ray transitions produced in the ^{92}Mo(^{83}Kr, $p3n$)^{171}Ir fusion-evaporation reaction [39] are also shown in Fig. 4. The results are included in Table 1. As can be seen in Fig. 4, the previously reported ground-state band transitions of ^{172}Pt up to $I^\pi = 8^+$ have positive asymmetry values and angular distribution ratios ($R_A = I(\theta \approx 140°)/I(\theta \approx 90°) \approx 1$) confirming that they have stretched electric quadrupole character and connecting a positive-parity $\Delta I = 2$ level sequence, as expected. The polarization and angular distribution measurements also show that the 769 keV transition has a stretched electric dipole character, unambiguously determining the spin and parity of the 1839 keV state to be 5^-.

The relative intensities of the $3^- \rightarrow 0^+$ and $3^- \rightarrow 2^+$ transitions enable us to calculate the ratio of the reduced E1 and E3 transition strengths from the 3^- state to be $B(E1 : 3^- \rightarrow 2^+)/B(E3 : 3^- \rightarrow 0^+) = 82(21) \times 10^{-12}\text{fm}^{-4}$. Systematics of known $B(E1)$ values for even–even nuclei in the vicinity of ^{172}Pt in the nuclear chart are shown in Fig. 5. We have also calculated a weighted average of the B(E1) values for all the transitions $\sim 3.4 \times 10^{-6}$ W.u.

Table 1 Experimental values for γ-ray transition energies (E_γ), initial level excitation energy (E_x), relative γ-ray intensities (I_γ), angular distribution ratios (R_A) and spin-parity assignments measured in this work for ^{172}Pt. New γ-ray transitions and new level excitation energies are indicated by an asterisk in the first and second column, respectively. The dagger symbol indicates a self-coincident doublet observed in the $\gamma - \gamma$ analysis. Statistical uncertainties are given in parentheses

E_γ (keV)	E_x (keV)	I_γ	R_A	$J_i^\pi \rightarrow J_f^\pi$
133.6(6)*	3127.8(7)*	2(1)		
149.4(5)*	2080.8(5)	3(1)		
184.3(3)	3177.2(5)*	3(1)		
213.0(1)	2955.7(6)	10(1)		
241.7(2)	2080.8(5)	20(2)	0.958(40)	$7_1^- \rightarrow 5_1^-$
250.7(5)*	2994.2(3)	3(1)		
293.1(2)	3035.7(6)*	6(1)		
324.5(2)	2406.2(2)	3(1)		
327.1(4)*	2080.8(5)	< 1		
336.6(2)†	2742.7(6)*	39(2)		$(9_1^-) \rightarrow 8_1^+$
353.8(3)*	3530.9(6)*	< 1		
366.0(2)	4921.0(5)*	3(1)		$(17_1^+) \rightarrow (16_1^+)$
373.5(2)	1839.1(4)	3(1)	1.063(328)	$5_1^- \rightarrow 3_1^-$
395.5(3)*	1465.6(4)	< 1		$3_1^- \rightarrow 4_1^+$
403.0(4)*	3991.4(5)*	< 1		
410.6(3)	3991.4(5)*	9(2)	1.211(55)	$(14_1^+) \rightarrow (12_1^+)$
434.4(4)*		< 1		
438.0(4)*		2(1)		
446.7(4)*		4(2)		
457.6(1)	457.6(1)	100(5)	0.935(16)	$2_1^+ \rightarrow 0_1^+$
463.4(4)*	2994.2(3)	4(2)		
474.1(3)*	2406.2(2)	2(1)		
496.0(2)		3(1)		
522.3(2)	3558.1(7)*	10(1)		
530.0(2)	2283.7(3)*	3(1)		
548.0(3)*	3290.7(7)*	2(1)		
563.6(2)	4555.0(5)*	4(1)		$(16_1^+) \rightarrow (14_1^+)$
567.1(3)	2742.7(6)*	11(2)		
573.3(4)*	2654.1(6)*	6(1)		
586.7(2)†	3580.8(3)	14(2)	0.965(37)	$(12_1^+) \rightarrow (10_1^+)$
588.0(2)†	2994.2(3)	15(2)	0.965(37)	$(10_1^+) \rightarrow 8_1^+$
594.2(2)*	3588.4(4)*	3(1)		
598.2(4)*		< 1		
612.5(1)†	1070.1(1)	106(5)	0.924(16)	$4_1^+ \rightarrow 2_1^+$
637.4(3)	5192.4(6)*	2(1)		$(18_1^+) \rightarrow (16_1^+)$
646.5(2)*	3177.2(5)*	< 1		
652.5(1)	2406.2(2)	52(2)	0.989(33)	$8_1^+ \rightarrow 6_1^+$
661.9(4)	2742.7(6)*	10(1)		$(9_1^-) \rightarrow 7_1^-$
676.6(2)*	4234.7(7)*	5(1)		
683.6(1)	1753.7(2)	78(3)	1.001(24)	$6_1^+ \rightarrow 4_1^+$
702.4(3)*	2986.1(4)*	< 1		
733.0(4)*		2(1)		
737.5(3)*	4972.2(8)*	3(1)		
766.6(2)*	5738.8(8)*	2(1)		
769.1(2)	1839.1(4)	35(2)	0.667(24)	$5_1^- \rightarrow 4_1^+$
777.0(4)*	2530.7(4)*	6(1)		
862.2(4)	1932.3(4)	8(1)		

Table 1 continued

E_γ (keV)	E_x (keV)	I_γ	R_A	$J_i^\pi \rightarrow J_f^\pi$
921.1(3)*	3001.9(6)*	2(1)		
956.1(3)*		2(1)		
1008.0(5)	1465.6(4)	4(1)	0.624(65)	$3_1^- \rightarrow 2_1^+$
1465.6(4)*	1465.6(4)	0.25(2)		$3_1^- \rightarrow 0_1^+$

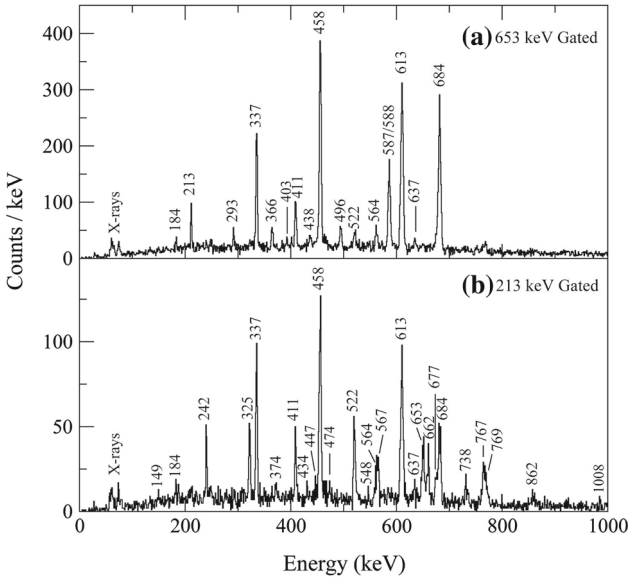

Fig. 2 Coincidence γ-ray energy spectra produced by gating on transitions in **a** the ground state band and **b** the negative-parity side band in the RDT-selected $\gamma - \gamma$ coincidence matrix

$(6.92 \times 10^{-6} e^2 \mathrm{fm}^2)$. Taking these measured $B(E1)$ values as a benchmark for the B(E1) strength in ^{172}Pt and using the Weisskopf estimates, one would expect a $B(E3 : 3^- \rightarrow 0^+)$ value of about 48(13) W.u., i.e. a transition to be potentially strongly collective.

4 Discussion

The presence of a low-lying negative-parity side band connected to the ground-state band with strong E1 transitions and a low-lying 3^- state which is depopulated by a $3^- \rightarrow 0^+$ E3 transition in competition with the $3^- \rightarrow 2^+$ E1 decay indicates strong octupole correlations in ^{172}Pt. This is somewhat surprising, given that ^{172}Pt, with 78 protons and 94 neutrons, is situated relatively far from the nearest "octupole-magic" number 88 in the nuclear chart and might indicate a new region of octupole softness that has not received attention until now. In order to investigate whether a low-lying 3^- state could alternatively be understood as a single-particle excitation rather than a collective octupole-vibrational state we have performed large-scale shell model (LSSM) calculations for ^{172}Pt and neighbouring Os and W isotopes between N = 82 and 94 using realistic nucleon–nucleon interactions. We considered ^{132}Sn as the inert core and included all neutron levels between N = 82 and 126 in the model space. Proton–proton and neutron–neutron interactions were taken from Refs. [46,47]. The cross-shell neutron–proton interactions were taken from the charge-dependent Bonn nucleon–nucleon potential with slight modifications in order to better reproduce the properties of the N = 84 isotones [48]. Given the large model space the calculations are computationally extremely challenging and it is to our knowledge the first time that detailed shell model calculations have been carried out for such heavy nuclear systems situated relatively far away from closed shells. The LSSM calculations reproduce reasonably well the excitation energies as well as the $B(E2; 2_1^+ \rightarrow g.s.)$ values for these nuclei. In order to study the spectrum of ^{172}Pt with a particular focus on the relative excitation energies of the yrast positive-parity states and the lowest negative-parity states we have calculated the lowest five states for each spin-parity up to 20^+ and 21^-. To facilitate the calculation and reduce the dimension of the model space, the maximum number of neutrons that can be excited to the $1f_{5/2}, 2p_{3/2}, 2p_{1/2}$, and $i_{13/2}$ orbitals was limited to two. The proton model space is truncated by limiting the excitations from $g_{7/2}$ and $d_{5/2}$ by considering the fact that the proton excitations are dominated by couplings within the $h_{11/2}$, $s_{1/2}$ and $d_{3/2}$ subshells. Part of the results are shown in Fig. 6. The theoretically predicted level energies are generally lower than the observed levels. However, a reasonable agreement between experiment and theory is obtained for the relative excitation energies of the yrast and near-yrast states with the notable exception of the 3^- state, which is experimentally observed to be situated much lower in excitation energy relative to the low-lying yrast positive-parity states compared with the LSSM prediction. As a comparison, we also did calculation with the original Kuo-Herling interaction [49]. The agreement with experiment is relatively worse in that calculation than that given in Fig. 6, even though the predicted energy (1.695 MeV) for the 6^+ state is much closer to experiment. The calculation based on the Kuo-Herling interaction also significantly overestimates the energy of the 3^- state. In the LSSM calculation the 3^- and 5^- states can be formed by a superposition of neutron $(i_{13/2}, f_{7/2})$ and proton $(h_{11/2}, d_{5/2})$ particle-hole excitations. These states

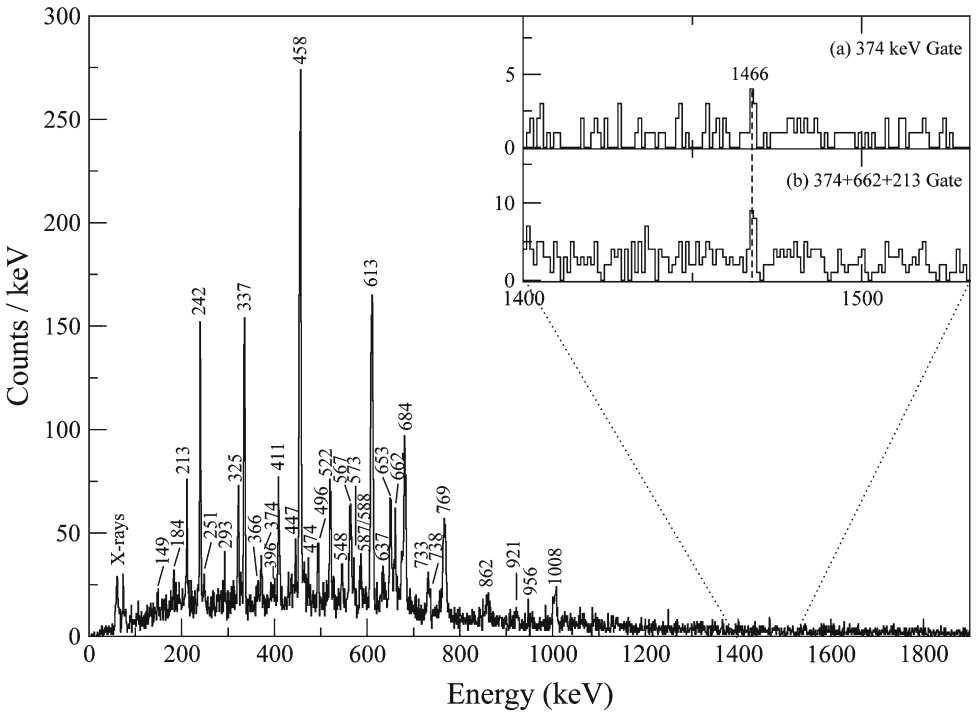

Fig. 3 Combined coincidence γ-ray energy spectrum produced from the sum of gates on the 374, 662 and 213 keV transitions in the $\gamma - \gamma$ matrix. The 1466 keV transition is highlighted in the insets by using **a** 374 keV gated spectrum and **b** a combination of 374, 662, and 213 keV gated spectra. The strongest transitions are marked with their energy in keV

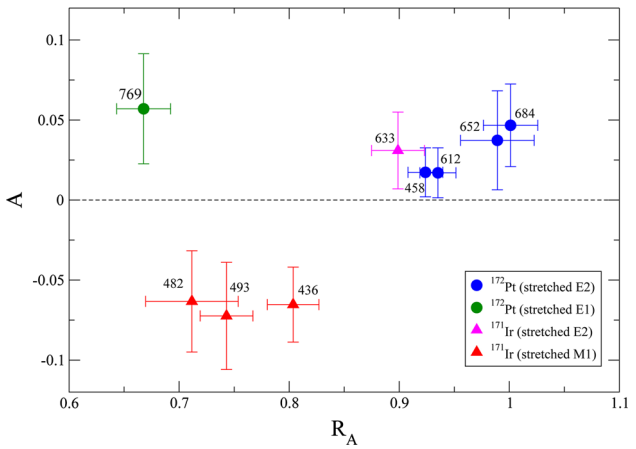

Fig. 4 Asymmetry parameter (A) versus angular distribution ratio (R_A) of γ rays deduced from the present work. The stretched E2 and E1 transitions in ^{172}Pt are shown as blue and green circles, respectively. A few stretched E2 and stretched M1 transitions belonging to ^{171}Ir [39] are shown as pink and red triangles, respectively

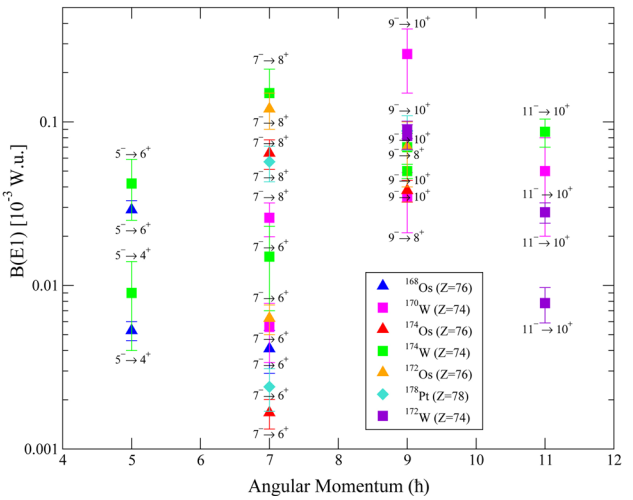

Fig. 5 Systematics of known $B(E1)$ values for nuclei in the vicinity of ^{172}Pt as a function of initial angular momentum of the decaying state. The data are taken from [40] (^{168}Os), [41] (^{170}W), [42] (^{172}W), [42] (^{172}Os), [43] (^{174}W), [44] (^{174}Os), [45] (^{178}Pt)

are predicted to be mainly of non-collective character. On the other hand, the experimentally observed lowest-lying 3^- state for which the predicted energy is significantly overestimated by both LSSM calculations, is likely to have a strong octupole-vibrational character which can bring down the energy of the state. At the present time it is very challenging, due to computation limitations, to reproduce such collective configurations even within the LSSM framework since they can only be generated by cross-major-shell excitations.

In order to investigate this possibility further we performed Woods-Saxon total Routhian surface (TRS) calculations based on the cranked Strutinsky formalism [50] for the ground-state and lowest-lying negative-parity configurations in ^{172}Pt. The results are shown in Fig. 7.

The calculations indicate octupole softness in the weakly quadrupole-deformed ($\beta_2 \approx 0.14$) ground-state minimum and show a pronounced octupole-deformed minimum for the lowest-lying negative-parity configuration with $\beta_3 \approx 0.05$, at the same quadrupole deformation. The negative-parity con-

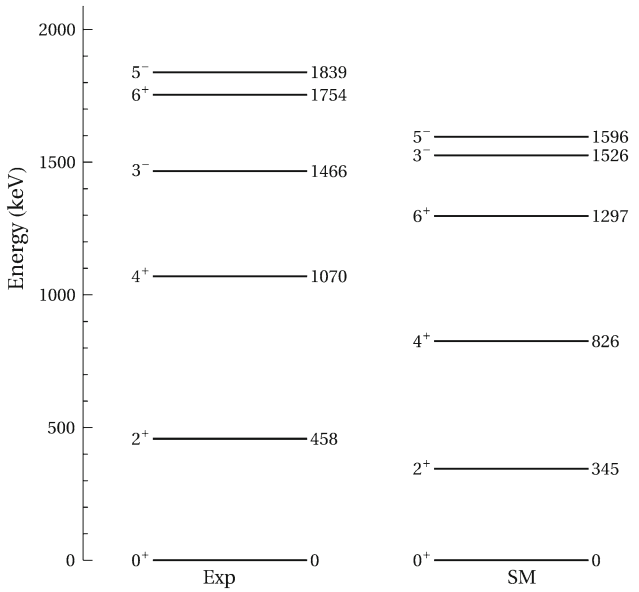

Fig. 6 Comparison between experimentally observed low-lying energy levels and shell model predictions for ^{172}Pt. Energies are given in keV

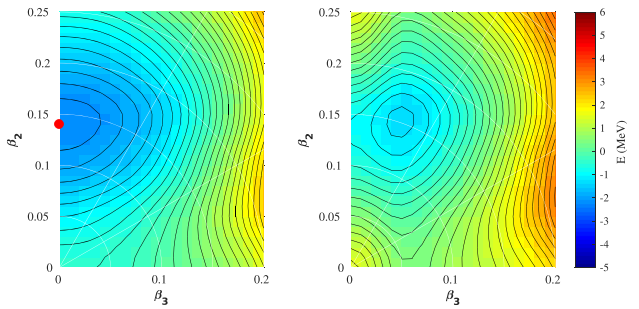

Fig. 7 Potential energy surfaces in the $\beta_2 - \beta_3$-plane for the vacuum (ground-state) configuration (left) and the lowest negative-parity configuration (right) in ^{172}Pt. The red dot indicates the position of the ground-state minimum. The equipotential energy lines below 6 MeV are displayed and the separation between neighboring energy lines is 200 keV

figuration, which corresponds to a neutron two-quasiparticle state, is calculated to be 1.113 MeV above the ground state. The negative-parity configuration also exhibits some β_3-softness with a saddle point at $\beta_3 = 0.0$, i.e. it satisfies the classical conditions for a system susceptible to octupole vibrations. The potential energy of the octupole-deformed minimum is also, interestingly, quite close to the observed excitation energy of the 3^- state. We therefore conclude that the experimental evidence for an octupole-vibrational 3^- state in ^{172}Pt is well supported by the TRS calculations as well as by the much higher relative excitation energy of the lowest-energy 3^- single-particle state predicted by our LSSM calculations. Further studies of octupole correlations in this region of the Segré chart are indicated, in particular a lifetime measurement for the 3^- state in ^{172}Pt is of paramount interest in order to measure the absolute collective strength of the $3^- \rightarrow 0^+$ transition.

5 Summary

Excited states in the extremely neutron deficient nucleus ^{172}Pt have been populated in heavy-ion fusion evaporation reactions and studied using the JUROGAM and GREAT spectrometers in conjunction with the RITU gas filled recoil separator. We report the observation of new excited states in ^{172}Pt, extending information on its structure compared with previous studies. Linear polarization and angular distribution measurements enabled firm spin-parity assignments for some of the most strongly populated states including the firm assignment of negative parity to an excited band structure feeding into the ground-state band with strong stretched E1 transitions. The observation of an E3 transition de-exciting the 3^- state at 1466 keV to the ground state and the presence of several E1 transitions connecting the negative-parity structure built on this state with the ground-state band provides strong evidence of octupole collectivity in ^{172}Pt. The experimental observations are supported by large-scale shell model calculations and potential energy surface calculations.

Acknowledgements Open access funding provided by Royal Institute of Technology. The authors thank the staff at the Accelerator Laboratory at the University of Jyväskylä for excellent technical support. This work was supported through EURONS (European Commission Contract no. RII3-CT-2004-506065) and by the Academy of Finland under the Finnish Centre of Excellence Programme. Further support for this work has been provided by the Swedish Research Council under Grant no. 621-2014-5558 and the United Kingdom Science and Technology Facilities Council. DMC, MG acknowledge support of the STFC under contract numbers EP/E02551X/1 and ST/L005794/1. E. I., Y. D. F., and M. K. R. acknowledge support from the International Joint Research Promotion Program of Osaka University and JSPS KAKENHI Grant number JP 17H02893. The authors acknowledge the support from the GAMMAPOOL detector collaboration for the loan of JUROGAM detectors.

Data Availability Statement This manuscript has no associated data or the data will not be deposited. [Authors' comment: All data generated during this study are contained in this published article.].

References

1. S.G. Nilsson, I. Ragnarsson, *Shapes and Shells in Nuclear Structure* (Cambridge University Press, Cambridge, 1995)
2. F. Asaro, F.S. Stephens, I. Perlman, Phys. Rev. **92**, 1495 (1953)
3. F.S. Stephens, F. Asaro, I. Perlman, Phys. Rev. **96**, 1568 (1954)
4. F.S. Stephens, F. Asaro, I. Perlman, Phys. Rev. **100**, 1543 (1955)
5. L.P. Gaffney et al., Nature **497**, 199 (2013)
6. H.J. Wollersheim et al., Nucl. Phys. A **556**, 261 (1993)
7. B. Bucher et al., Phys. Rev. Lett. **116**, 112503 (2016)
8. B. Bucher et al., Phys. Rev. Lett. **118**, 152504 (2017)
9. P.A. Butler et al., Nat. Commun. **10**, 2473 (2019)
10. P.A. Butler, W. Nazarewicz, Rev. Mod. Phys. **68**, 349 (1996)
11. G.A. Leander, W. Nazarewicz, G.F. Bertsch, J. Dudek, Nucl. Phys. A **453**, 58 (1986)
12. R.J. Poynter et al., Phys. Lett. B **232**, 447 (1989)
13. G. De Angelis et al., Phys. Lett. B **535**, 93 (2002)
14. P. Kleinheinz et al., Z. Phys. A **286**, 27 (1978)
15. M. Piiparinen et al., Phys. Rev. Lett. **70**, 150 (1993)
16. H. Mach et al., Phys. Rev. C **42**, R811 (1990)
17. P. Moller, J.R. Nix, Nucl. Phys. A **361**, 117 (1981)
18. W. Nazarewicz et al., Nucl. Phys. A **429**, 269 (1984)
19. J. Skalski et al., Phys. Lett. B **238**, 6 (1990)
20. I. Ahmad, P.A. Butler, Annu. Rev. Nucl. Part. Sci. **43**, 71 (1993)
21. E.S. Paul et al., Phys. Rev. C **51**, 78 (1995)
22. R.S. Simon et al., Z. Phys. A **325**, 197 (1986)
23. F. Beck et al., Prog. Part. Nucl. Phys. **28**, 443 (1992)
24. C. Beausang, J. Simpson, J. Phys. G **22**, 527 (1996)
25. R.D. Page et al., Nucl. Instrum. Methods B **204**, 634 (2003)
26. M. Leino et al., Nucl. Instrum. Methods B **99**, 653 (1995)
27. M. Leino, Nucl. Instrum. Methods B **126**, 320 (1997)
28. J. Sarén, J. Uusitalo, M. Leino, J. Sorri, Nucl. Instrum. Methods Phys. A **654**, 508 (2011)
29. B. Cederwall et al., Phys. Rev. Lett. **121**, 022502 (2018)
30. M.J. Taylor et al., Nucl. Instrum. Methods Phys. Res. Sec. A **707**, 143 (2013)
31. C.W. Beausang et al., Nucl. Instrum. Methods A **313**, 37 (1992)
32. I.H. Lazarus et al., IEEE Trans. Nucl. Sci. **48**, 567 (2001)
33. P. Rahkila, Nucl. Instrum. Methods Phys. Res. Sect. A **595**, 637 (2008)
34. D. Radford, Nucl. Instrum. Methods Phys. Res. Sect. A **361**, 297 (1995)
35. B. Cederwall et al., Phys. Lett. B **443**, 69 (1998)
36. D. Seweryniak et al., Phys. Rev. C **58**, 2710 (1998)
37. M. Danchev et al., Phys. Rev. C **67**, 014312 (2003)
38. D.T. Joss et al., Phys. Rev. C **74**, 014302 (2006)
39. R. Bark et al., Nucl. Phys. A **657**, 113 (1999)
40. T. Grahn et al., Phys. Rev. C **94**, 044327 (2016)
41. C.M. Baglin et al., Nucl. Data Sheets **153**, 417–436 (2018)
42. B. Singh, Nucl. Data Sheets **75**, 340–365 (1995)
43. E. Browne, H. Junde, Nucl. Data Sheets **87**, 141–147 (1999)
44. J. Gascon et al., Nucl. Phys. A **470**, 230–240 (1987)
45. E. Achterberg, O.A. Capurro, G.V. Marti, Nucl. Data Sheets **110**, 14731688 (2009)
46. C. Qi, Z.X. Xu, Phys. Rev. C **86**, 044323 (2012)
47. C. Qi, L.Y. Jia, G.J. Fu, Phys. Rev. C **94**, 014312 (2016)
48. R.J. Carroll et al., Phys. Rev. C **94**, 064311 (2016)
49. J.B. McGrory, T.T.S. Kuo, Nucl. Phys. A **247**, 283–316 (1975)
50. W. Satula, R. Wyss, Phys. Scr. T **56**, 159 (1995)